The Astrophysical Journal, 700:302–308, 2009 July 20 doi:10.1088/0004-637X/700/1/302


# ON THE SPIN–ORBIT MISALIGNMENT OF THE XO-3 EXOPLANETARY SYSTEM*

Joshua N. Winn[1], John Asher Johnson[2,10], Daniel Fabrycky[3], Andrew W. Howard[4], Geoffrey W. Marcy[4], Norio Narita[5], Ian J. Crossfield[6], Yasushi Suto[7], Edwin L. Turner[8,9], Gil Esquerdo[3], and Matthew J. Holman[3]
[1] Department of Physics, and Kavli Institute for Astrophysics and Space Research, Massachusetts Institute of Technology, Cambridge, MA 02139, USA
[2] Institute for Astronomy, University of Hawaii, Honolulu, HI 96822, USA
[3] Harvard-Smithsonian Center for Astrophysics, 60 Garden Street, Cambridge, MA 02138, USA
[4] Department of Astronomy, University of California, Mail Code 3411, Berkeley, CA 94720, USA
[5] National Astronomical Observatory of Japan, Osawa, Mitaka, Tokyo 181-8588, Japan
[6] Department of Astronomy, University of California, 430 Portola Plaza, Box 951547, Los Angeles, CA, USA
[7] Department of Physics, The University of Tokyo, Tokyo 113-0033, Japan
[8] Princeton University Observatory, Princeton, NJ 08544, USA
[9] Institute for the Physics and Mathematics of the Universe, University of Tokyo, Kashiwa, Chiba 277-8568, Japan
*Received 2009 February 17; accepted 2009 May 19; published 2009 July 1*

## ABSTRACT

We present photometric and spectroscopic observations of the 2009 February 2 transit of the exoplanet XO-3b. The new data show that the planetary orbital axis and stellar rotation axis are misaligned, as reported earlier by Hébrard and coworkers. We find the angle between the sky projections of the two axes to be $37.3 \pm 3.7$ deg, as compared to the previously reported value of $70 \pm 15$ deg. The significance of this discrepancy is unclear because there are indications of systematic effects. XO-3b is the first exoplanet known to have a highly inclined orbit relative to the equatorial plane of its parent star, and as such it may fulfill the predictions of some scenarios for the migration of massive planets into close-in orbits. We revisit the statistical analysis of spin–orbit alignment in hot-Jupiter systems. Assuming the stellar obliquities to be drawn from a single Rayleigh distribution, we find the mode of the distribution to be $13^{+5}_{-2}$ deg. However, it remains the case that a model representing two different migration channels—in which some planets are drawn from a perfectly aligned distribution and the rest are drawn from an isotropic distribution—is favored over a single Rayleigh distribution.

*Key words:* planetary systems – planetary systems: formation – stars: individual (XO-3, GSC 03727-01064) – stars: rotation

*Online-only material:* machine-readable table

## 1. INTRODUCTION

Many exoplanets have eccentric orbits. It is widely held that the orbits were initially circular, due to dissipation in the protoplanetary disk, and that the eccentricities were somehow excited after the planets acquired most of their mass. It is also presumed that orbits were initially aligned with the protoplanetary disk, which was itself aligned with the equatorial plane of the parent star. Whether this alignment is generally maintained is not obvious; whatever mechanism excites the orbital eccentricities may also perturb the orbital inclinations. For example, large eccentricities may be produced by close encounters between planets (Rasio & Ford 1996; Weidenschilling & Marzari 1996; Lin & Ida 1997), which would occasionally produce large inclinations, even if the initial inclinations are only a few degrees (Chatterjee et al. 2008).

For close-in giant planets ("hot Jupiters") in particular, which are thought to have formed at large orbital distances and then migrated inward, one may wonder whether the migration process disturbed the original coplanarity. The various migration theories differ on this point. Migration via tidal torques from the protoplanetary disk should not excite the inclination, and may even drive the system toward closer alignment (Lubow & Ogilvie 2001). In contrast, migration via planet–planet scattering would magnify any initial misalignments (Chatterjee et al. 2008; Nagasawa et al. 2008; Jurić & Tremaine 2008). Scenarios involving Kozai cycles can also leave a highly inclined final state (Wu et al. 2007; Fabrycky & Tremaine 2007; Nagasawa et al. 2008). Thus, one might learn about a planet's migration history by seeking evidence for a tilt of its orbit with respect to the stellar equatorial plane.

For transiting planets, spin–orbit alignment is assessed by observing the Rossiter–McLaughlin (RM) effect, a time-dependent distortion in the stellar spectral-line profile due to the partial eclipse of the rotating stellar photosphere. The distortion is usually manifested as an anomalous Doppler shift during transits. It was first observed in an exoplanetary system by Queloz et al. (2000) and has since been observed in more than a dozen systems. The theory and applications of the RM effect have also been discussed extensively (Ohta et al. 2005; Giménez 2006; Gaudi & Winn 2007; Fabrycky & Winn 2009).

Analysis of the RM effect allows one to determine $\lambda$, the angle between the sky projections of the orbital axis and the stellar rotation axis. All exoplanets that have been examined—with two exceptions—have been found to be consistent with close alignment and small values of $\lambda$. One exception was HD 17156b, for which Narita et al. (2008) found $\lambda = 62 \pm 25$ deg, but follow-up observations by Cochran et al. (2008) and Barbieri et al. (2008) showed good alignment (as also confirmed by N. Narita et al. 2009). The other exception is XO-3b, for which Hébrard et al. (2008; hereafter H08) found $\lambda = 70 \pm 15$ deg based on observations with the 1.93 m telescope at the

* Data presented herein were obtained at the W. M. Keck Observatory, which is operated as a scientific partnership among the California Institute of Technology, the University of California, and the National Aeronautics and Space Administration, and was made possible by the generous financial support of the W. M. Keck Foundation.
[10] NSF Astronomy and Astrophysics Postdoctoral Fellow.

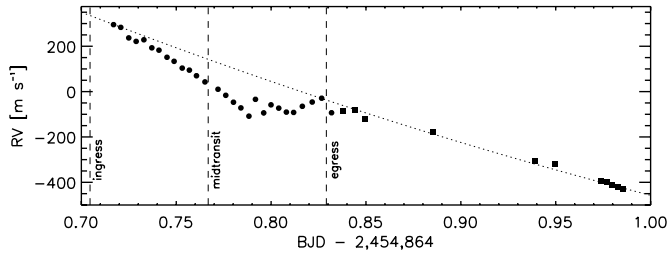


**Figure 1.** Apparent radial velocity variation of XO-3 during the 2009 February 2 transit, based on observations with Keck/HIRES. The internal measurement errors are smaller than the symbol sizes. Dashed lines indicate the photometrically determined times of ingress, midtransit, and egress. The dotted line is the model of the orbital RV variation described in Section 3.2.

Observatoire de Haute-Provence (OHP) and the SOPHIE spectrograph (Bouchy & The Sophie Team 2006). However, those authors cautioned that additional data were needed to exclude the possibility that the Doppler measurements were affected by systematic errors related to the high airmass and bright sky background of some of their observations.

In this paper, we present more definitive data for XO-3, based on simultaneous spectroscopic and photometric observations of the transit of 2009 February 2. We describe the observations and data reduction procedures in Section 2. In Section 3, we present evidence for spin–orbit misalignment by modeling the RM effect. In Section 4, we discuss the results and some of their implications.

## 2. OBSERVATIONS

### 2.1. Spectroscopy

We observed the transit of UT 2009 February 2 with the Keck I 10 m telescope on Mauna Kea, Hawaii. We used the High Resolution Echelle Spectrometer (HIRES; Vogt et al. 1994) in the standard setup of the California Planet Search program, as summarized here. We employed the red cross-disperser and used the $I_2$ absorption cell to calibrate the instrumental response and the wavelength scale. The slit width was 0.″86 and the typical exposure time was 300 s, giving a resolution of 65,000 and a signal-to-noise ratio (S/N) of 110 pixel$^{-1}$.

We obtained 39 spectra over 6.5 hr. The observations began just before 12° twilight, during the transit ingress. They continued throughout the 2.5 hr transit and for 0.5 hr after egress. Over the next 3.5 hr we observed other targets, returning several times to XO-3 to measure the orbital radial velocity (RV) variation as precisely as possible. We determined the relative Doppler shifts with the algorithm of Butler et al. (1996). Measurement errors were estimated from the scatter in the solutions for each 2 Å section of the spectrum. The data are given in Table 1 and plotted in Figure 1.

### 2.2. Photometry

Simultaneous photometric observations of the 2009 February 2 transit were conducted with the 1.2 m telescope at the Fred L. Whipple Observatory (FLWO) in Arizona, and the Nickel 1 m telescope at Lick Observatory in California. At FLWO we used Keplercam, a $4096^2$ CCD with a 23′ square field of view. The images were binned $2\times2$, giving a scale of 0.″68 per binned pixel. We obtained 15 s exposures though an *r*-band filter for 5.5 hr bracketing the predicted midtransit time. At Lick Observatory we used the Nickel Direct Imaging Camera, which has a $2048^2$ CCD with a 6.″3 square field of view. The images were binned $2\times2$, giving a scale of 0.″37 per binned pixel. We used a Cousins *I* filter, and an exposure time between 7 and 9 s depending on the conditions.

The CCD images were reduced using standard IRAF[11] procedures for bias subtraction, flat-field division, and aperture photometry. The flux of XO-3 was divided by a weighted sum of the fluxes of comparison stars elsewhere in the field of view. Corrections were applied to account for systematic effects due to differential extinction and imperfect flat fielding, using a procedure described in Section 3.1. The final time series of relative flux measurements are given in Table 2, and plotted in Figure 2. The FLWO data have a median time between samples of 29 s and an out-of-transit standard deviation of 0.0020. For the Lick data, the corresponding numbers are 22 s and 0.0022.

**Table 1**
Relative Radial Velocity Measurements of XO-3

| BJD | RV (m s$^{-1}$) | Error (m s$^{-1}$) |
|---|---|---|
| 2454864.71696 | 295.28 | 8.47 |
| 2454864.72077 | 283.24 | 9.22 |
| 2454864.72498 | 236.89 | 8.63 |
| 2454864.72887 | 221.36 | 8.68 |
| 2454864.73296 | 228.46 | 8.29 |
| 2454864.73714 | 193.07 | 8.10 |
| 2454864.74090 | 182.65 | 8.45 |
| 2454864.74513 | 151.37 | 8.58 |
| 2454864.74887 | 133.62 | 8.85 |
| 2454864.75315 | 103.70 | 9.28 |
| 2454864.75693 | 94.67 | 8.10 |
| 2454864.76066 | 69.94 | 9.39 |
| 2454864.76514 | 42.68 | 9.49 |
| 2454864.77202 | 10.35 | 8.11 |
| 2454864.77610 | −16.32 | 8.98 |
| 2454864.78016 | −46.80 | 8.49 |
| 2454864.78408 | −71.76 | 8.12 |
| 2454864.78831 | −108.26 | 9.64 |
| 2454864.79175 | −34.11 | 9.40 |
| 2454864.79610 | −93.81 | 10.74 |
| 2454864.79994 | −58.44 | 9.33 |
| 2454864.80403 | −72.96 | 9.37 |
| 2454864.80804 | −90.44 | 9.62 |
| 2454864.81188 | −91.84 | 9.02 |
| 2454864.81646 | −64.90 | 8.79 |
| 2454864.82167 | −46.12 | 8.89 |
| 2454864.82664 | −29.13 | 9.05 |
| 2454864.83185 | −93.29 | 9.95 |
| 2454864.83813 | −84.01 | 9.20 |
| 2454864.84428 | −83.04 | 7.95 |
| 2454864.84934 | −121.17 | 9.76 |
| 2454864.88547 | −179.66 | 8.36 |
| 2454864.93909 | −307.71 | 8.57 |
| 2454864.94942 | −320.68 | 9.57 |
| 2454864.97407 | −394.97 | 9.24 |
| 2454864.97694 | −397.80 | 8.71 |
| 2454864.97973 | −413.02 | 8.65 |
| 2454864.98273 | −420.18 | 9.08 |
| 2454864.98550 | −431.56 | 9.46 |

**Notes.** The RV was measured relative to an arbitrary template spectrum; only the differences are significant. The uncertainty given in Column 3 is the internal error only and does not account for any possible "stellar jitter."

[11] IRAF is distributed by the National Optical Astronomy Observatories, which is operated by the Association of Universities for Research in Astronomy, Inc., under cooperative agreement with the National Science Foundation.

**Table 2**
Relative Photometry of XO-3

| Observatory[a] | BJD | Rel. Flux | Error |
|---|---|---|---|
| 1 | 2454864.62513 | 0.9995 | 0.0020 |
| 1 | 2454864.62544 | 1.0011 | 0.0020 |
| 1 | 2454864.62579 | 0.9997 | 0.0020 |
| 1 | 2454864.62612 | 1.0008 | 0.0020 |
| 1 | 2454864.62646 | 1.0015 | 0.0020 |
| 1 | 2454864.62678 | 0.9985 | 0.0020 |
| 1 | 2454864.62712 | 1.0007 | 0.0020 |
| 1 | 2454864.62743 | 1.0006 | 0.0020 |

**Note.** [a] (1) FLWO 1.2 m telescope, *r* band. (2) Nickel 1 m telescope, *I* band.

(This table is available in its entirety in a machine-readable form in the online journal. A portion is shown here for guidance regarding its form and content.)

## 3. DATA ANALYSIS

### *3.1. Determination of the Midtransit Time*

As long as a transiting planet's trajectory (the "transit chord") does not pass too close to the center of the stellar disk, a condition that is fulfilled for XO-3b, the value of $\lambda$ is mainly encoded in the time difference between the transit midpoint and the moment when the anomalous Doppler shift vanishes. The main purpose of the new photometry was to determine the precise midtransit time. The other photometric parameters, such as the transit duration and depth, have already been determined by Johns-Krull et al. (2008) and Winn et al. (2008; hereafter JK08 and W08, respectively) with uncertainties that are negligible for our purposes.

We fitted a model to each photometric time series in which the free parameters were the midtransit time $T_c$ and some parameters relating to systematic effects that were evident in the data. For the FLWO data, the parameters were $m_0$ and $k_z$ describing a correction due to differential extinction,

$$m_{\rm cor} = m_{\rm obs} + m_0 - k_z z, \quad (1)$$

where $m_{\rm obs}$ is the observed magnitude, $z$ is the airmass, and $m_{\rm cor}$ is the corrected magnitude that is compared to an idealized Mandel & Agol (2002) model. For the Lick data, a strong correlation was also found between the out-of-transit flux and the $x$ and $y$ pixel coordinates of XO-3, presumably due to imperfect flat-field calibration. For these data the correction took the form

$$m_{\rm cor} = m_{\rm obs} + m_0 - k_x x - k_y y - k_z z. \quad (2)$$

All of the other relevant parameters were held fixed at the values determined by W08. To determine the allowed ranges of the parameters, we used a Markov Chain Monte Carlo (MCMC) algorithm.[12] For the FLWO data, we assumed the photometric errors to be Gaussian with a standard deviation equal to the observed out-of-transit standard deviation. We did the same for the Lick data, except that we further multiplied the error bars by 1.8 to correct for time-correlated noise. The factor of 1.8 was determined by examining the standard deviation of progressively time-binned light curves; for averaging times between 10 and 20 minutes, the standard deviation exceeds the expectation of uncorrelated Gaussian noise by a factor of 1.8 (for further discussion, see Section 3 of W08).

[12] Tegmark et al. (2004), Ford (2005), and Gregory (2005) provide useful background information on this method. For our particular implementation, see, e.g., Holman et al. (2006) or Winn et al. (2007a).

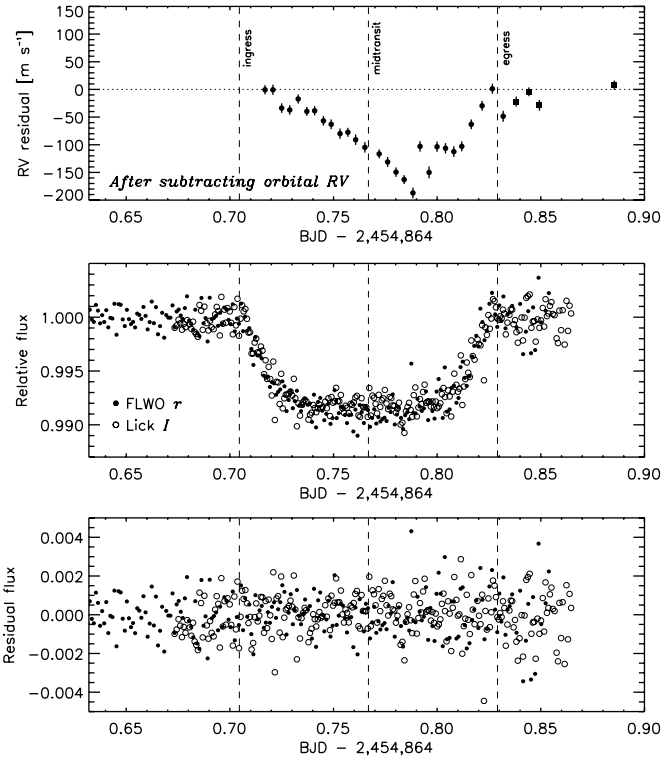


**Figure 2.** Spectroscopic and photometric observations of XO-3 during the 2009 February 2 transit. Top: the same data as in Figure 1, after subtracting the orbital RV model (see Section 3.2). The error bars represent internal measurement errors only and do not include "stellar jitter." Middle: relative photometry based on *r*-band observations with the FLWO 1.2 m telescope and *I*-band observations with the Nickel 1 m telescope. The data have been binned ×3 for display purposes. Bottom: differences between the photometric data and the best-fitting model.

Based on the W08 ephemeris, the predicted midtransit time was Barycentric Julian Date (BJD) $2454864.7663 \pm 0.0010$. The FLWO result for the midtransit time, expressed in fractional days after BJD 2454864, is $0.76668 \pm 0.00051$. The Lick result is $0.76787 \pm 0.00079$. The difference between the FLWO and Lick results is $102 \pm 81$ s, suggesting that our error bars are reasonable. We refined the transit ephemeris by including the two new data points in the compilation of JK08 and W08 and fitting a linear function $T_c[N] = T_c[0] + NP$, where $N$ is an integer. The linear fit gave $\chi^2 = 30.7$ with 29 degrees of freedom. Figure 3 shows the timing residuals. The refined ephemeris is

$$T_c[0] = 2,454,864.76684 \pm 0.00040 \text{ BJD}$$
$$P = 3.1915289 \pm 0.0000032 \text{ days}. \quad (3)$$

### *3.2. Evidence for Spin–Orbit Misalignment: Simple Analysis*

The apparent radial velocity variation seen in Figure 1 arises from both orbital motion and the RM effect. To remove the variation due to orbital motion and isolate the RM effect, we determined the parameters of the best-fitting Keplerian orbital model based on 20 RV measurements published by H08, and then subtracted the orbital model from the Keck data. Specifically, we used the 19 RVs gathered at essentially random orbital phases outside of transits during the few weeks after the transit observation of 2008 January 28. We also used one data point from 2008 January 28 that was obtained before the transit began.

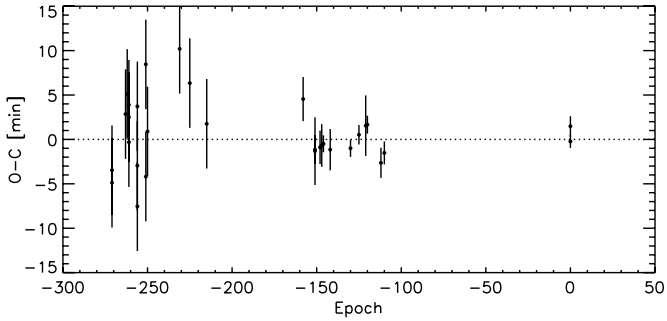


**Figure 3.** Transit timing residuals. A linear function of epoch was fitted to the transit times of JK08, W08, and this work, and the calculated times were subtracted from the observed times. The data from the XO Survey instruments were not used.

Our MCMC algorithm found the best values and uncertainties of the velocity semiamplitude $K$, orbital eccentricity $e$, argument of pericenter $\omega$, systemic velocity $\gamma$, orbital period $P$, and midtransit time $T_c$. Gaussian prior constraints were imposed on $P$ and $T_c$ based on Equation (3), and uniform priors were used for the other parameters. The results were consistent with the results of H08 but with greater precision in $P$ and $T_c$. We fixed $\{K, e, \omega, P, T_c\}$ at their optimized values, and found the choice of $\gamma$ that best fits the out-of-transit Keck data (indicated by square symbols in Figure 1). Then we subtracted the model from the Keck data. The results are shown in the top panel of Figure 2.

For a prograde orbit with well aligned spin and orbital axes, one expects the RM anomaly to be positive (redshifted) for the first half of the transit, because the planet is blocking a portion of the approaching (blueshifted) half of the rotating star. Then one expects the RM anomaly to vanish at midtransit, when the planet is in front of the projected stellar rotation axis. Finally, in the last half of the transit, one expects the RM anomaly to be negative (blueshifted) because the planet is blocking a portion of the receding (redshifted) half of the rotating star.

Figure 2 does not show this pattern. Instead, the anomaly is a blueshift from at least one-quarter of the way into the transit until its completion. Based on a linear fit to the data from the first half of the transit, the RM anomaly vanished $\Delta t = 72 \pm 9$ minutes before the transit midpoint. Evidently, the planet passed in front of the projected rotation axis before it reached the midpoint of the transit chord. This can happen only if the sky-projected rotation axis and the normal to the transit chord are misaligned.[13] Thus, without detailed modeling of the RM effect, we may conclude that the orbit of XO-3b is inclined with respect to the rotation axis of its parent star.

If we may approximate the planet's motion across the stellar disk as uniform and rectilinear, then from the geometry of the transit chord we may relate $\Delta t$ to $\lambda$:

$$\frac{\Delta t}{T} = \frac{b \tan \lambda}{2\sqrt{1 - b^2}}, \quad (4)$$

where $b$ is the transit impact parameter in units of the stellar radius and $T$ is the total transit duration, with endpoints defined by the passage of the center of the planet over the stellar limb. Using $b$ and $T$ from W08, and $\Delta t = 72 \pm 9$ minutes from the preceding analysis, we find $\lambda = 44 \pm 4$ deg.

[13] Or equivalently, if the transit chord is misaligned with the "projected stellar equator," defined as the stellar diameter that is perpendicular to the projected rotation axis.

Although this calculation has the virtue of simplicity, it is unsatisfactory in some respects. It relies on an extrapolation to determine the time when the RM anomaly vanished. The uncertainty in the orbital model is not taken into account. Also neglected are the nonuniform motion of the planet across the stellar disk, and the slight misalignment between the projected orbital axis and the normal to the transit chord. Furthermore, the information conveyed by amplitude and duration of the RM waveform is ignored.

### *3.3. Evidence for Spin–Orbit Misalignment: Comprehensive Analysis*

A better model includes a simultaneous description of the orbital motion and the RM effect. The orbital motion is described by a Keplerian RV curve, as in Section 3.2. To model the RM effect, it is necessary to establish the relation between the anomalous RV and the configuration of the star and planet. For this purpose, we used the procedure described by Winn et al. (2005): we simulated RM spectra with the same format and noise characteristics as the actual data, and determined the apparent RV using the same algorithm used on the actual data.

The premise of the simulation is that the only relevant variations in the emergent spectrum across the visible stellar disk are those due to uniform rotation and limb darkening. Variations due to differential rotation, turbulent motion, convective cells, and other effects are neglected. We begin with a template spectrum with minimal rotational broadening (described below). We apply a rotational broadening kernel with $v \sin i_\star = 18.5$ km s$^{-1}$ to mimic the disk-integrated spectrum of XO-3.[14] Then we subtract a scaled, velocity-shifted version of the original narrow-lined spectrum, intended to represent the portion of the stellar disk hidden by the planet. We perform this step for many choices of the scaling $\delta$ and velocity shift $V_p$, and then we "measure" the anomalous Doppler shift $\Delta V_R$ of each spectrum. A polynomial function is fitted to the relation between $\Delta V$ and $\{\delta, V_p\}$.

The template spectrum should be similar to that of XO-3 but with comparatively little rotational broadening. We used a Keck/HIRES spectrum of HD 3861 (F5V, $v \sin i_\star = 2.8$ km s$^{-1}$; Valenti & Fischer 2005) with an S/N of 500 and a resolution of 70,000. Based on the results we adopted the following relation:

$$\Delta V_R = -\delta V_p \left[ 1.644 - 1.036 \left( \frac{V_p}{18.5 \text{ km s}^{-1}} \right)^2 \right]. \quad (5)$$

The complete RV model is $V_O(t) + \Delta V_R(t)$, where $V_O$ is the line-of-sight component of the Keplerian orbital velocity and $\Delta V_R$ is the Rossiter anomaly given by Equation (5), with $\delta$ from the Mandel & Agol (2002) model and $V_p$ computed under the assumption of a uniformly rotating photosphere. The Keplerian orbit is parameterized by the period $P$, time of transit $T_c$, velocity semiamplitude $K$, eccentricity $e$, argument of pericenter $\omega$, and a constant additive velocity $\gamma$. The RM effect is parameterized by the projected stellar rotation rate $v \sin i_\star$ and the projected spin–orbit angle $\lambda$.

We fitted the 39 Keck velocities presented in Section 2.1 and the 20 OHP out-of-transit velocities of H08 that were specified in Section 3.2. The OHP out-of-transit data were included to constrain the Keplerian orbital parameters. The OHP transit data were *not* included, thereby allowing the Keck data to provide

[14] Here and elsewhere, we use $i_\star$ to denote the inclination of the stellar rotation axis with respect to the sky plane. This is to be contrasted with $i_o$, the inclination of the orbital axis with respect to the sky plane.

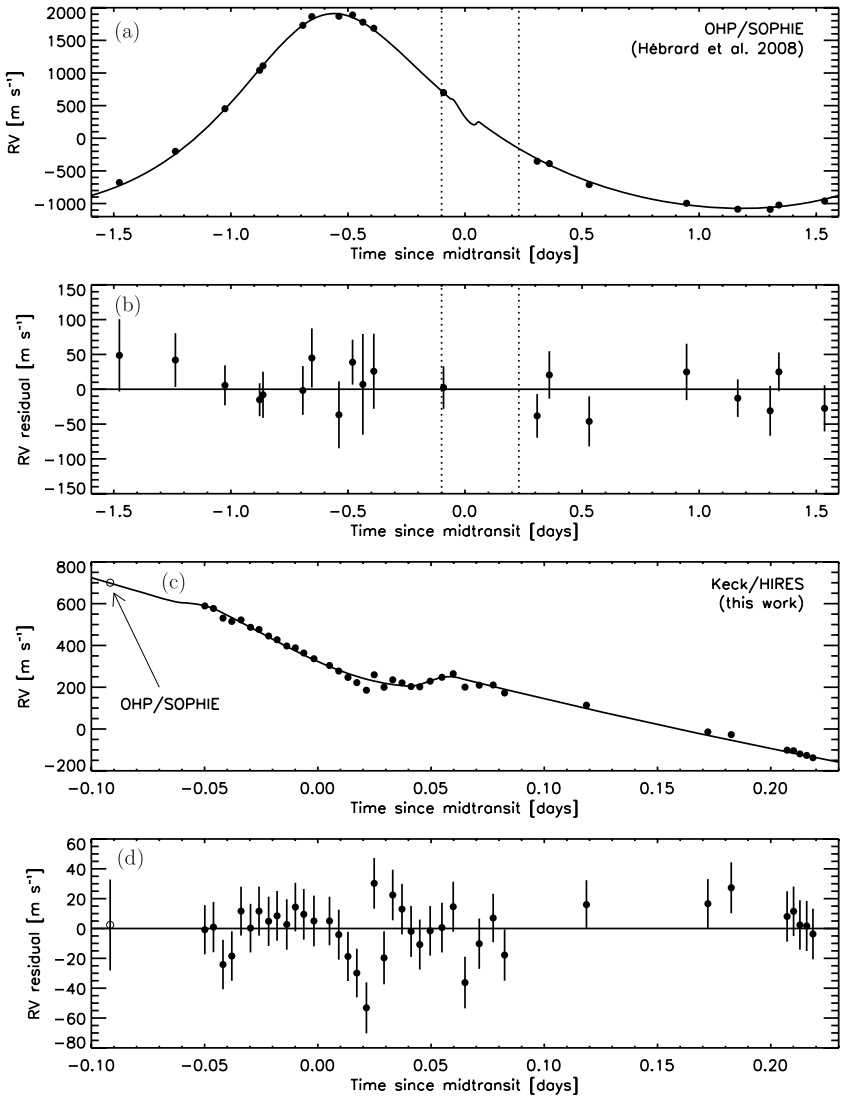


**Figure 4.** Radial velocity model including orbital motion and the RM effect. (a) The H08 data. The solid curve is the best-fitting model. The dotted lines indicate the time range plotted in the lower two panels. (b) Differences between the H08 data and the best-fitting model. (c) The Keck/HIRES data from the transit of 2009 February 2. Also plotted is the single point from H08 that was used in the model-fitting procedure. (d) Differences between the Keck/HIRES data and the best-fitting model. The error bars are the quadrature sums of the internal measurement error and 14.1 m s$^{-1}$ (the "stellar jitter" term).

an independent determination of the transit parameters $\lambda$ and $v \sin i_\star$. The OHP and Keck data were granted independent values of $\gamma$.

We determined the credible intervals for the model parameters with an MCMC algorithm. Uniform priors were used for $K$, $e \cos \omega$, $e \sin \omega$, $\gamma_{\rm OHP}$, $\gamma_{\rm Keck}$, $v \sin i_\star$, and $\lambda$. Gaussian priors were used for $P$ and $T_c$, based on the ephemeris of Equation (3). For the parameters needed to compute the fractional loss of light $\delta$, namely the transit depth, total duration, and duration of ingress or egress, we used Gaussian priors based on the results of W08.[15] We found it necessary to enlarge the RV errors by adding 14.1 m s$^{-1}$ in quadrature with the measurement errors in order to achieve a reduced $\chi^2$ of unity. This is a plausible level of intrinsic velocity noise ("stellar jitter") for an F5V star, based on the empirical findings of Wright (2005).

[15] An additional parameter with a minor role is the linear limb-darkening coefficient $u$ that is used to compute $\delta$. We set $u = 0.5$ based on the expectation for a star such as XO-3 in the red optical band (Claret 2004). Varying this parameter by as much as $\pm 0.3$ or even allowing it to be a free parameter makes no essential difference in the results.

The results for the model parameters are given in Table 3. The quoted value for each parameter is the median of the a posteriori distribution, marginalized over all other parameters. The quoted $1\sigma$ (68.3% confidence) errors are defined by the 15.85% and 84.15% levels of the cumulative distribution. Our results for $K$, $e$, $\omega$, and $\gamma_{\rm OHP}$ are in accord with the previous analysis of H08, the only differences having arisen from our choice of priors on $P$ and $T_c$. As expected, the results for the photometric parameters were very close to the Gaussian prior constraints that were imposed. The best-fitting model is shown in Figure 4.

Through this analysis we found $\lambda = 37.3 \pm 3.7$ deg. A similar result was obtained in Section 3.2 using a naïve model, although we have already noted some shortcomings of the simple analysis. The comprehensive model takes into account the nonuniform orbital velocity, as well as all other relevant information and uncertainties in the external parameters. It also gives an independent estimate of the projected stellar rotation rate, $v \sin i_\star = 18.31 \pm 1.3$ km s$^{-1}$. There is good agreement with the value determined from the stellar line-broadening,

**Table 3**
Radial Velocity Model Results for XO-3

| Parameter | Value | Uncertainty |
|---|---|---|
| Projected spin–orbit angle, $\lambda$ (deg) | 37.3 | 3.7 |
| Projected stellar rotation rate, $v \sin i_\star$ (km s$^{-1}$) | 18.31 | 1.3 |
| Velocity semiamplitude, $K$ (m s$^{-1}$) | 1488 | 10 |
| Orbital eccentricity, $e$ | 0.2884 | 0.0035 |
| Argument of pericenter, $\omega$ (deg) | 346.3 | 1.3 |
| Velocity offset, $\gamma_{\rm Keck}$ (m s$^{-1}$) | −293.6 | 7.0 |
| Velocity offset, $\gamma_{\rm OHP}$ (m s$^{-1}$) | −12045.4 | 8.0 |

$18.54 \pm 0.17$ km s$^{-1}$ (JK08), which is a consistency check on our interpretation of the RV data and our model of the RM effect.

## 4. DISCUSSION

Through simultaneous photometry and spectroscopy of a transit of XO-3b, we have determined that the planetary orbit is significantly inclined relative to the equatorial plane of its host star. According to our analysis, the angle between the sky projections of the orbital axis and the stellar rotation axis is $\lambda = 37.3 \pm 3.7$ deg. Thus, we have confirmed the finding of H08 that XO-3b is the first known case of an exoplanet whose orbit is highly inclined with respect to the equatorial plane of its parent star, or equivalently, the first exoplanetary system in which the host star is known to have a large obliquity.

Quantitatively, our result for $\lambda$ disagrees with the previous result ($70 \pm 15$ deg) by $2.1\sigma$, where $\sigma$ is the quadrature sum of the errors in the two results. The significance of this discrepancy is small and its interpretation is unclear. It is possible the systematic effects over which H08 expressed concern, due to high airmass and moonlight, have biased the result for $\lambda$. It is also possible we are underestimating the error in $\lambda$ by assuming the RV errors to be Gaussian and uncorrelated. The Keck RV residuals do not appear to be Gaussian and uncorrelated; in particular, the four largest outlying data points were all from the narrow time range between 0.02 and 0.04 days after midtransit. The noise may include artifacts of the instrument or data reduction procedures, or sources of apparent radial velocity variation besides Keplerian orbital motion and the RM effect—such as star spots, other activity-induced variations, and additional planets—that are correlated on the timescale of the transit. The best way to reduce this source of uncertainty is to gather more spectroscopic transit data, preferably covering an entire transit and including plenty of pre-ingress and post-egress data.

Because the angle $i_\star$ is unknown, the projected spin–orbit angle $\lambda = 37.3 \pm 3.7$ deg gives a lower limit on the true angle $\psi$ between the orbital axis and the stellar rotation axis. Thus, the orbit of XO-3b is more inclined relative to its host star than any planet in the solar system, including Pluto ($\psi = 12.2$ deg).

The unknown angle $i_\star$ is also relevant to the determination of the stellar rotation period $P_{\rm rot}$. Using the estimates of $R_\star$ and $v \sin i_\star$ by W08 and JK08,

$$P_{\rm rot} = \frac{2\pi R_\star}{v \sin i_\star} \sin i_\star = (3.73 \pm 0.23 \text{ d}) \sin i_\star. \quad (6)$$

This is not far from the orbital period of 3.19 d and thus it is possible that the spin and orbit are synchronized, or pseudo-synchronized (H08). However, tidal theory would predict that such a system would have a fleeting existence, for the following reasons. Tidal evolution does not lead to a stable equilibrium configuration for most of the star–planet pairs, possibly including XO-3 (Rasio et al. 1996; Levrard et al. 2009). Even if the star were tidally spun up, it would be expected to lose angular momentum through a wind and consequently consume the planet (Barker & Ogilvie 2009). Furthermore, the dissipation in the star that would drive its spin into pseudosynchronization with the orbit would also damp the orbital eccentricity on a similar timescale, because the ratio of orbital to spin angular momentum is small (Hut 1981). Hence, the observation of a significant eccentricity suggests that the stellar spin has not been significantly altered by tides. However, some other systems present circumstantial evidence for tidal spin–orbit interactions (McCullough et al. 2008; Pont 2009).

The large obliquity of its host star is not the only unusual property of XO-3b. Even by the standards of hot Jupiters it is an outlier, with an unusually large mass ($12\,M_{\rm Jup}$) and orbital eccentricity ($e = 0.29$). Naturally one wonders if there is a connection between these properties and the nonzero value of $\lambda$, as mentioned in the introduction. There are at least two other massive planets on close-in eccentric orbits which have been subjects of RM observations, and in both cases $\lambda$ has been found to be consistent with zero: HAT-P-2b (Winn et al. 2007b; Loeillet et al. 2008) and HD 17156b (Cochran et al. 2008; Barbieri et al. 2008; Narita et al. 2009).[16] Is XO-3b anomalous even within the subgroup of close-in massive planets on eccentric orbits? The answer is not yet clear. It must be remembered that the RM effect is sensitive only to the projected spin–orbit angle and it is therefore possible that the other systems are also significantly misaligned; this is especially so for HAT-P-2b because the small impact parameter of the transit degrades the achievable precision in $\lambda$.

Fabrycky & Winn (2009) presented a framework for overcoming the problem of projection effects using a Bayesian analysis of the results from many different planets. They found that the conclusions that could be drawn from the current ensemble were strongly driven by the case of XO-3b. Specifically, they compared two descriptions of the data: (1) a model in which a fraction $f$ of systems have perfect spin–orbit alignment and the rest have random mutual orientations; (2) a model in which the spin–orbit angle $\psi$ is drawn from a Rayleigh distribution (or more precisely a Fisher distribution on a sphere, which reverts to a Rayleigh distribution when it is highly directional). They calculated the Bayesian evidence

$$E \equiv \int p(\text{data}|\alpha)\, p(\alpha)\, d\alpha \quad (7)$$

for each model, where $\alpha$ is the single free parameter of the model (either the fraction $f$, or the mode $\sigma$ of the Rayleigh distribution). They found $E$ to be 134 times greater for the first model, a finding that was interpreted as evidence for two distinct modes of planet migration. However, they cautioned that this conclusion hinged on the tentative finding of $\lambda = 70 \pm 15$ deg for XO-3.

We have repeated this analysis using the revised estimate of $\lambda = 37.3 \pm 3.7$ deg and making no other changes. Results from the first model, a division between perfectly aligned and randomly oriented systems, remain nearly the same: $f < 0.36$ with 95% confidence, and the Bayesian evidence $E$ is 1920 (having fallen only slightly from 1927). Results from the second

[16] Moutou et al. (2009) recently reported observations of the RM effect in the highly eccentric HD 80606 system. The authors did not determine $\lambda$ because their data only cover the latter part of the transit, but they found that the data are compatible with a large spin–orbit misalignment if the orbital inclination is not too close to 90°.

model changed more significantly. The reduced value of $\lambda$ for XO-3 makes a single Rayleigh distribution more probable, with $E = 69$ instead of 14. In addition, with the improved precision of the new result, $\lambda = 0$ is ruled out with higher confidence, leading to a sharper lower limit on the mode $\sigma$ of the Rayleigh distribution. We find $\sigma = 13^{+5}_{-2}$ deg ($1\sigma$ errors). In this model, the most probable value of $\psi$ among hot-Jupiter systems is larger than the value of 6 deg between the solar rotation axis and Jupiter's orbital axis. The first model is preferred, with a formal confidence of $E_1/(E_1 + E_2) = 96.6\%$. However, the confidence has been reduced from the value of 99.28% calculated by Fabrycky & Winn (2009). Thus, although the evidence for two wholly distinct modes of planet migration has been weakened, it is still highly suggestive.

As with many attempts to derive conclusions based on a posteriori statistics, a problem with the foregoing analysis is that subtle and ill-quantified selection effects have shaped the sample under consideration. In particular, XO-3b was not selected randomly for this study. The previous finding of a large value of $\lambda$ was a motivating factor that has led to improved precision in $\lambda$, and consequently greater weight in the statistical analysis. Furthermore, the idea to fit a model consisting of two distributions (perfectly aligned and isotropic) was developed only after knowing of XO-3's possibly strong misalignment.

Apart from those thorny issues, the high sensitivity of the statistical results to a single data point means that the results must be treated with caution, and underlines the importance of gathering additional data. Observing more transits of XO-3b is advisable, given the possibility noted earlier of correlated RV noise. Observations of the RM effect are also desired for other transiting systems, spanning a range of planetary masses, orbital eccentricities, and orbital periods. Such observations would elucidate any connections between the planetary and orbital parameters, and may provide important clues about the processes that lead to close-orbiting planets.

We thank Peter McCullough for reminding us about the near-coincidence of the orbital and rotational periods of XO-3b. We are grateful to Gáspár Bakos for trading telescope time at FLWO on short notice, and to Breann Sitarski and Tracy Ly for helping with the observations at Lick Observatory. We are indebted to Lara Winn for enabling this work to be completed in a timely fashion. This work was partly supported by the NASA Origins program through awards NNX09AD36G and NNX09AB33G. J.A.J. acknowledges support from an NSF Astronomy and Astrophysics Postdoctoral Fellowship (grant AST-0702821). This work was partly supported by World Premiere International Research Center Initiative (WPI Initiative), MEXT, Japan.

## REFERENCES

Barbieri, M., et al. 2008, arXiv:0812.0785
Barker, A. J., & Ogilvie, G. I. 2009, MNRAS, 395, 2268
Bouchy, F., & The SOPHIE Team 2006, in Tenth Anniversary of 51 Peg-b: Status of and Prospects for Hot Jupiter Studies, ed. L. Arnold, F. Bouchy, & C. Moutou (Paris: Frontier Group), 319
Butler, R. P., Marcy, G. W., Williams, E., McCarthy, C., Dosanjh, P., & Vogt, S. S. 1996, PASP, 108, 500
Chatterjee, S., Ford, E. B., Matsumura, S., & Rasio, F. A. 2008, ApJ, 686, 580
Claret, A. 2004, A&A, 428, 1001
Cochran, W. D., Redfield, S., Endl, M., & Cochran, A. L. 2008, ApJ, 683, L59
Fabrycky, D., & Tremaine, S. 2007, ApJ, 669, 1298
Fabrycky, D. C., & Winn, J. N. 2009, ApJ, 696, 1230
Ford, E. B. 2005, AJ, 129, 1706
Gaudi, B. S., & Winn, J. N. 2007, ApJ, 655, 550
Giménez, A. 2006, ApJ, 650, 408
Gregory, P. C. 2005, ApJ, 631, 1198
Hébrard, G., et al. 2008, A&A, 488, 763 (H08)
Holman, M. J., et al. 2006, ApJ, 652, 1715
Hut, P. 1981, A&A, 99, 126
Johns-Krull, C. M., et al. 2008, ApJ, 677, 657 (JK08)
Jurić, M., & Tremaine, S. 2008, ApJ, 686, 603
Levrard, B., Winisdoerffer, C., & Chabrier, G. 2009, ApJ, 692, L9
Lin, D. N. C., & Ida, S. 1997, ApJ, 477, 781
Loeillet, B., et al. 2008, A&A, 481, 529
Lubow, S. H., & Ogilvie, G. I. 2001, ApJ, 560, 997
Mandel, K., & Agol, E. 2002, ApJ, 580, L171
McCullough, P. R., et al. 2008, arXiv:0805.2921
Moutou, C., et al. 2009, A&A, 498, L5
Nagasawa, M., Ida, S., & Bessho, T. 2008, ApJ, 678, 498
Narita, N., Sato, B., Ohshima, O., & Winn, J. N. 2008, PASJ, 60, L1
Narita, N., et al. 2009, PASJ, in press (arXiv:0905.4727)
Ohta, Y., Taruya, A., & Suto, Y. 2005, ApJ, 622, 1118
Pont, F. 2009, MNRAS, in press (arXiv:0812.1463)
Queloz, D., Eggenberger, A., Mayor, M., Perrier, C., Beuzit, J. L., Naef, D., Sivan, J. P., & Udry, S. 2000, A&A, 359, L13
Rasio, F. A., & Ford, E. B. 1996, Science, 274, 954
Rasio, F. A., Tout, C. A., Lubow, S. H., & Livio, M. 1996, ApJ, 470, 1187
Tegmark, M., et al. 2004, Phys. Rev. D, 69, 103501
Valenti, J. A., & Fischer, D. A. 2005, ApJS, 159, 141
Vogt, S. S., et al. 1994, Proc. SPIE, 2198, 362
Weidenschilling, S. J., & Marzari, F. 1996, Nature, 384, 619
Winn, J. N., Holman, M. J., & Roussanova, A. 2007a, ApJ, 657, 1098
Winn, J. N., et al. 2005, ApJ, 631, 1215
Winn, J. N., et al. 2007b, ApJ, 665, L167
Winn, J. N., et al. 2008, ApJ, 683, 1076 (W08)
Wright, J. T. 2005, PASP, 117, 657
Wu, Y., Murray, N. W., & Ramsahai, J. M. 2007, ApJ, 670, 820